



Calhoun: The NPS Institutional Archive

Faculty and Researcher Publications

Faculty and Researcher Publications Collection

1992-05

Sliding Mode Acoustic Servoing for an Autonomous Underwater Vehicle

Marco, D.B.

Offshore Technology Conference

<http://hdl.handle.net/10945/48945>



Calhoun is a project of the Dudley Knox Library at NPS, furthering the precepts and goals of open government and government transparency. All information contained herein has been approved for release by the NPS Public Affairs Officer.

Dudley Knox Library / Naval Postgraduate School
411 Dyer Road / 1 University Circle
Monterey, California USA 93943

<http://www.nps.edu/library>



OTC 6974

Sliding Mode Acoustic Servoing for an Autonomous Underwater Vehicle

D.B. Marco and A.J. Healey, Naval Postgraduate School

Copyright 1992, Offshore Technology Conference

This paper was presented at the 24th Annual OTC in Houston, Texas, May 4-7, 1992.

This paper was selected for presentation by the OTC Program Committee following review of information contained in an abstract submitted by the author(s). Contents of the paper, as presented, have not been reviewed by the Offshore Technology Conference and are subject to correction by the author(s). The material, as presented, does not necessarily reflect any position of the Offshore Technology Conference or its officers. Permission to copy is restricted to an abstract of not more than 300 words. Illustrations may not be copied. The abstract should contain conspicuous acknowledgment of where and by whom the paper is presented.

Abstract

Currently in use at the Naval Postgraduate School is a fully functional experimental autonomous underwater vehicle (AUV). The vehicle serves as a test bed for research in autonomous control, autonomous obstacle avoidance, automatic fault detection, guidance and control at slow speed. It measures over seven feet (two meters) in length and weighs about 430 pounds (215 kg). Maneuvering control is provided by four rudders and dive planes, has twin propulsion motors, and onboard sensors for speed, depth, angular rates and positions and four ultrasonic sensors for range information. All shipboard action is controlled by a 68030 microprocessor running under an OS-9 operating system and a G-96 bus with code written in 'C' language. All systems are powered by lead acid gell batteries for a test mission duration of about two hours.

This paper presents some experimental modeling results upon which computer simulations of the dynamic positioning performance are based. Details are given of the vehicle modeling, the influence of thruster dynamic lags, Sliding Mode control design including integral control for the compensation of ocean current effects, and a Kalman filter design for the estimation of target range and velocity from noisy sonar data. The filter can remove transient fault anomalies which are common in sonar data.

References and illustrations at end of paper

Introduction

This paper provides an analysis of the effects of ocean current, thruster dynamic lags and acoustic sensor noise on the motion control of an underwater vehicle in the longitudinal direction. The context and importance of this work lies in the increased use of ROV's for deep ocean intervention and inspection tasks. With the ever increasing emphasis on reduction of costs, it is the contention of the authors that the use of fully autonomous vehicles will be needed for routine underwater jobs because they can be deployed from platforms and will not need the support of expensive surface assets. One of the missions foreseen for vehicles of this type is to provide inspection of underwater facilities. Motion control using onboard sonar to 'servo' to a target will be a typical operation.

Current research at NPS and elsewhere is aimed at designing robust controllers for underwater vehicles, the slow speed behavior of which are highly uncertain. The robust control of ROV's has been addressed by Yoerger and Slotine (1985), and the design and operation of the Jason supervisory control system has been described by Yoerger et. al. (1986), in which a surface operator drives the vehicle using a manual teleoperated link from a surface ship. More recently, Fossen (1991) has studied the same subject. At NPS we are exploring the behavior of fully autonomous underwater vehicles which are programmed prior to launch and for which there is no tether. After recovery,

the data stored on board is uploaded for data visualization and postprocessing. All mission functions are controlled by the onboard autonomous controller. The ability to control the vehicle motion near an underwater target is critical, and this is made more difficult by the presence of ocean currents, dynamic lags in the operation of the thrusters as shown by Yoerger et. al. (1991), and sensor noise from the onboard sonar ranging devices.

The paper gives an outline of the dynamic model used for longitudinal motion control of an underwater vehicle; the design procedure for a sliding mode position controller including the use of integral control for reduction of steady state position control errors when ocean currents can not be precisely known; and the influence of thruster lags which act to destabilize the motion. Added sensor noise from sonar devices is modelled and filtered using a Kalman filter to estimate the vehicle's motion. While the paper is based on simulated results, experiments with the NPS AUV II vehicle are being conducted in order to verify the contentions provided herein.

Vehicle Modeling

The equations of motion of underwater vehicles appear in other places as in Abkowitz (1965), Principles of Naval Architecture (1967), and, more recently with specific reference to underwater vehicle simulation and control by Healey (1992), and neglecting the effects of sway, yaw, heave, pitch, and roll, may be expressed for the surge motion direction as:

$$\dot{u}(t) = -\alpha u(t)|u(t)| + \beta n(t)|n(t)| \dots\dots\dots(1)$$

with the global velocity, given by;

$$\dot{x}(t) = u(t) + u_{cx} \dots\dots\dots(2)$$

where $u(t)$ is the surge velocity of the vehicle relative to a coordinate frame located in the ocean body of water, moving with current velocity u_{cx} in the longitudinal direction. $n(t)$ represents the vehicle propulsion system propellor rotational speed, and α is a coefficient representing the combined effects of vehicle body drag as well as the effect of loss of propulsion force with vehicle forward motion speed. The propellor 'bollard pull' thrust depends on the square of the propellor rotation rate with a coefficient, β , given as,

$$\beta = \alpha[u_0 / n_0]^2$$

where

$$\alpha = \frac{\rho L^2 C_d}{[2m + \rho L^3 X_{\dot{u}}]}$$

m is the vehicle mass; C_d is the effective longitudinal drag coefficient, L is the vehicle length and ρ is the water density.

Notice that the vehicle longitudinal added mass is included in terms of the nondimensional positive coefficient $X_{\dot{u}}$ (assumed constant) with the vehicle's rigid body mass.

Appropriate values of α and β were determined by in water testing of the NPS AUV II vehicle with a speed command entered of 1.5 ft / sec. and using a Kalman filter for parameter identification. Figure 1 shows the vehicle and Figure 2 shows its response together with predicted model values for the acceleration behavior.

Sliding Mode Tracking Control Design

Global position tracking errors are defined in terms of the errors between actual and commanded position and velocity by,

$$\begin{aligned} \tilde{x}(t) &= x(t) - x_{com}(t) ; \\ \tilde{\dot{x}}(t) &= \dot{x}(t) - \dot{x}_{com}(t). \end{aligned} \dots\dots\dots(3)$$

Sliding Mode control, as described by Slotine and Coetsee (1986), and by Utkin (1977), selects a sliding surface $\sigma(t)$, that is either a stable polynomial operator acting on the output error, or a linear combination of the system state variables. The vehicle motion is in terms of the velocity $u(t)$ relative to the water, and here, the current u_{cx} acts as a disturbance producing a steady offset in the position control. This may be compensated by the use of integral control. Therefore, by contrast to other work, we add to the system of equations an additional equation defining the integral of position error as,

$$\dot{z}(t) = \tilde{x}(t) \dots\dots\dots(4)$$

with which we now define a sliding surface given by;

$$\sigma(t) = \ddot{z}(t) + \lambda_1 \dot{z}(t) + \lambda_2 z(t). \dots\dots\dots(5)$$

and by differentiation, the sliding surface can be computed in terms of position and velocity measurements as

$$\sigma(t) = \tilde{\dot{x}}(t) + \lambda_1 \tilde{x}(t) + \lambda_2 z(t) \dots\dots\dots(6)$$

The constants λ_1 and λ_2 must be chosen to provide a stable polynomial operator when $\sigma(t) = 0$ which represents the state of affairs when the vehicle response is in a sliding condition. With a control that will drive $\sigma(t)$ to zero, the positional error will be driven to zero. Now, even in the presence of disturbances which would tend to force $\sigma(t)$ to a nonzero constant, the positional error will be driven to zero while the integrator output will go to a non zero constant. To ensure global asymptotic stability of $\sigma(t)$, and a system return to a sliding condition from any initial condition or disturbed state, a Lyapunov function is formed in $\sigma(t)$ whose time derivative is always negative. The control to provide that condition will provide stable control of the vehicle. It follows that if we define

$$V = 0.5 \sigma^2(t)$$

asymptotic stability will be achieved if

$$\dot{V} = \sigma(t)\dot{\sigma}(t) < 0 \quad \forall t > 0 \quad \dots\dots\dots(7)$$

A more useful form of the above is to require that

$$\dot{\sigma}(t) = -\eta \text{sat}(\sigma(t) / \phi) \quad \dots\dots\dots(8)$$

The function $\text{sat}(\sigma(t)/\phi)$ is a saturation function modeled by

$$\begin{aligned} d\sigma(t)/dt &= -\eta \text{sign}(\sigma(t)) \quad |\sigma(t)| > \phi \\ d\sigma(t)/dt &= -\eta \sigma(t)/\phi \quad |\sigma(t)| < \phi \dots\dots\dots(9) \end{aligned}$$

The use of this smoothing function is to reduce control chatter which would otherwise occur with the sharp switching rule implied by (7) where $d\sigma(t)/dt$ is discontinuous at $\sigma(t)=0$. Substitution from (6) gives a formulation for the required control law using the vehicle dynamics as,

$$\begin{aligned} \alpha(\dot{x}(t) - u_{cx})|(\dot{x}(t) - u_{cx})| + \beta n(t)|n(t)| - \dot{x}_{com}(t) \\ + \lambda_1 \tilde{x}(t) + \lambda_2 \ddot{x}(t) = -\eta \text{sat}(\sigma(t) / \phi) \end{aligned}$$

$$n_2(t) = \ddot{x}_{com}(t) - \lambda_1 \tilde{x}(t) - \lambda_2 \ddot{x}(t)$$

$$-\alpha(\dot{x}(t) - u_{cx})|(\dot{x}(t) - u_{cx})| - \eta \text{sat}(\sigma(t) / \phi)$$

and so,

$$n(t) = \beta^{-1} \left\{ \sqrt{|n_2(t)|} \right\} \text{sign}(n_2(t)) \dots\dots\dots(10)$$

The usefulness of the Sliding Mode approach is that stability in the presence of certain levels of uncertainty can be verified. Uncertainty occurs in the modeling of β and α , and in the estimation of the ocean current. So, under closed loop conditions, an errors analysis may be

performed by substituting (10) into (1) and applying the result to equation (8) using (6). In this process, it is realized that the control law (10) must use erroneous estimates of the current \hat{u}_{cx} and the vehicle dynamics constants, so that cancelling like terms, the true system sliding surface dynamics are dependent on the estimation errors as in;

$$\dot{s}(t) = \delta f - \eta \tanh(\sigma(t) / \phi)$$

where the time dependent uncertainty is given by,

$$\begin{aligned} \delta f = \alpha(\dot{x}(t) - u_{cx})|(\dot{x}(t) - u_{cx})| \\ - \hat{\alpha}(\dot{x}(t) - \hat{u}_{cx})|(\dot{x}(t) - \hat{u}_{cx})| \end{aligned}$$

leading to a criterion that the switching strength, η , must be at least,

$$\eta > \|\delta f\|$$

to guarantee stability.

Integral Control and Wind Up

If the above conditions are met, then $d\sigma(t)/dt$ will approach zero and $\sigma(t)$ will tend to a constant value which is proportional to the mismatch in the estimate of the current. This effect is exactly the desired result, as the tendency of $\sigma(t)$ to a constant proportional to the current estimation mismatch, allows the positional error to be driven to zero as t tends to infinity - a design feature of the incorporation of integral control. While the elimination of steady state positional error is a desirable feature of integral control, one side problem is that, if unchecked, the integral variable $z(t)$ builds up in an unbounded way. Even if the steady state positional errors ultimately tend to zero, the large built up value in $z(t)$ takes a long time to reduce. This well known problem with integral control is called 'wind up'. It is eliminated by the introduction of a limit function essentially preventing the large build up of high values in $z(t)$. What is actually used in the formation of the sliding surface is a limited form of $z(t)$ given by;

$$\text{if } |z(t)| > z_{limit}, z(t) = z_{limit} * \text{sign}(z_{limit}) \dots(11)$$

The effectiveness of the suppression of integral control wind up will be demonstrated by the results of simulations later in this paper.

Incorporation of Thruster Lags

In order to more fully simulate the dynamic behavior of the vehicle, the effect of thruster lags are incorporated by a first order lagging response of actual thrust to changes in the propellor speed. τ is the first order time

constant, and the actual thrust is then modeled by $f_c(t)$ where

$$\dot{f}_c(t) = -[1/\tau]f_c(t) + [\beta/\tau]n(t)|n(t)| \dots(12)$$

When simulating thruster lags, a modification to equation (1) is then made as follows to be used with the model in equation (12).

$$\dot{u}(t) = -\alpha u(t)|u(t)| + f_c(t) \dots\dots\dots(13)$$

Sensor Noise and the Use of a Kalman Filter

Programing the control law given by equation (10) into a vehicle control computer requires the availability of signals corresponding to the estimate of the ocean current, the vehicle position relative to the target and the relative velocity between the vehicle and the target. These quantities are presumed to be available from ultrasonic sonars which, at best, give a noisy measurement of the required signals. Since a separate doppler sonar is not available on the NPS AUV II vehicle, estimates of position and velocity need to be extracted from the primary sonar range data. We assume a model based on kinematics where a three state filter is used corresponding to the estimated position, velocity and acceleration of the range signal and so the system model for the measurement process becomes,

$$\begin{aligned} \hat{x}(t) &= x_1(t) + q_1(t) \\ \dot{x}_1(t) &= x_2(t) + q_2(t) \dots\dots\dots(14) \\ \dot{x}_2(t) &= 0 + q_3(t) \end{aligned}$$

in which $\hat{x}(t)$, $x_1(t)$, $x_2(t)$, are estimates of the position, velocity and acceleration from the sonar range signal, $r(t)$. The measurement equation with $r(t)$ being the sonar ranger output signal becomes,

$$r(t) = \hat{x}(t) + v(t) \dots\dots\dots(15)$$

The values of the system noises, $q_1(t)$, $q_2(t)$, $q_3(t)$, and the measurement noise $v(t)$, must be estimated and the filter design and speed of response is dependent on the choices made. Generally, increasing the system noise values makes the filter faster in response with less filtering of the measurement noise and increasing the measurement noise produces the converse. The formulas for the updating of the position and velocity estimates are standard and are not repeated here. The effects of the use of the filter will be elucidated in the section on simulated results below.

Simulation Results

The results that follow are computer simulations based on the model given by equation (1) and (2) with the Sliding Mode Control given by equations (10). All responses are to a step input of 10.0 ft (3 meters) with a velocity and acceleration command of zero. Position and velocity commands consistent with a stepwise acceleration profile can be used to control the overshoot seen in Figure 3. The step input in position command was used to more fully show the transient behavior of the system. The initial velocity of the vehicle relative to the water is assumed to be zero as it is released into the current. The initial design of the Sliding Controller was based on values of 1.0 for λ_1 and λ_2 in rad/sec. and rad/sec² units respectively. The controller formulation used estimates of the position and velocity from the Kalman filter driven by the range signal corrupted by an estimate of the signal noise, $v(t)$.

Simulations were carried out using Matlab on Sun and Vax workstations. Experimental data were obtained from testbed runs of the NPS AUV II vehicle during the last year.

Figure 3 shows the vehicle position response and the resulting command for propellor speed from the Sliding Mode Controller incorporating integral control features as outlined in the sections above. Also shown for contrast, are results without integral control ($\lambda_2 = 0$). Perfect state measurements are assumed for this result without any sensor noise or thruster lags. The actual current simulated was - 4.0 ft/sec, while the estimated current used in the controller was -1.0 ft/sec. The need for integral control is clearly shown by the steady state offset present without the integral term. Using the integral formulation not only removes the offset, but the system speed of response is increased.

The values of $\sigma(t)$ along with certain terms of the sliding surface for the above results are shown in Figure 4. For the case with integral control, $\sigma(t)$ approaches the value of the term $\lambda_2 z(t)$, and for the case without integral control, $\sigma(t)$ approaches the value of the term $\lambda_1 \tilde{x}(t)$ and $\sigma(t)$ is the same value in the steady state regardless of which controller is used. Since the final position of the vehicle is constant, $\sigma(t)$ must be the same for the commanded speed to be identical from both controllers. This may be seen by inspection of equations (6) and (10), setting $\lambda_2 = 1$ and then to 0 to compare the steady state values of $n(t)$ for the two cases.

Figure 5 shows the effect of measurement noise on the position and propeller speed. A uniformly distributed random signal with zero mean was added to the position measurement prior to the Kalman filter estimation. The mismatch between the actual and estimated current for this simulation was reduced by setting $u_{cx} = -4.0$ and $\hat{u}_{cx} = -3.0$. The responses to noise amplitudes of 0.2 and then 0.5 feet is shown. The positioning performance is only slightly affected by the introduction of the noise. The propeller speed command on the other hand is highly affected by the measurement noise, increasing in amplitude with increased noise amplitude.

To investigate the effects of thruster lags, the position responses to three different values of the time constant, τ , in equation (12) is shown in Figure 6. A measurement noise amplitude of 0.5 feet is used. The response to $\tau = 0.2$ seconds is quite good, but becoming more oscillatory for $\tau = 0.5$ sec. The system becomes unstable when τ is increased to 1.0 sec. This demonstrates that the thruster lag can significantly change the behavior of the system and must be estimateable to some degree and compensated if it is large. Figure 7 shows the position and propulsion force response for the case of $\tau = 0.2$ sec.

So far, the simulations have used a fast acting controller and a fast Kalman filter. The fast controller implies that the term ϕ is relatively small. For our case $\phi = 1.0$. Figure 8 shows the position and propeller speed response for a slow controller with $\phi = 20.0$ and no measurement noise. The transient part of the response between 0 and about 12 seconds is independent of ϕ , since the switching term is saturated during this time. Near the target position, however, a small position offset is present, and is attributed to the small gain of the non-linear switching term. This significantly reduces the effectiveness of the integral term in the formulation of the sliding surface.

Since the Kalman filter is fast, the estimates of $x(t)$ and $\dot{x}(t)$, in the absence of measurement noise, have been very close to the actual values. If noise is present, the filter also faithfully reproduces the noise which causes the propeller commands to follow noisy measurements and produces undesirable chattering in the propellers (Figure 5). In an effort to remove this, the filter was slowed to provide smoother measurements for feedback to the controller. Figure 9 shows the actual values of $x(t)$ and $\dot{x}(t)$ along with the estimates from the Kalman filter for fast gains.

The figure clearly shows the effect of the noise in the estimated values which are generally larger in magnitude than the actual values. The phase lag on the other hand is quite small and permits a stable response of the system. Response to a much slower filter is shown in Figure 10. Smoothing of the noise has been accomplished, but the magnitude errors have grown along with a significant phase lag in the estimate of $\dot{x}(t)$. These errors, especially in the phase of the estimated global velocity, $x_1(t)$ has caused the system to become unstable. This demonstrates that the filter must be tuned so that noise effects are minimized while maintaining a reasonable estimate of the position and velocity.

Conclusions

A procedure to position an underwater vehicle in the presence of a current using acoustic servoing has been presented. Since the only method of position measurement was assumed to be from acoustic range sensors, a Kalman filter was needed to estimate the vehicle velocity from the range data. The inclusion of an integral term in the sliding surface formulation removes steady state position offsets caused by the current. Effects of lags between propeller speed and propulsion force were studied and it was confirmed, as expected, that system instability will occur if a large delay is present and uncompensated. Since acoustic sensors are often noisy, simulations including sensor noise were performed. The noise corrupted measurements cause the propeller speed to chatter when high gain controllers are used. If precision motion control is to be achieved, particular attention must be paid to improved modelling of thrusters, including their dynamic performance. Secondly, the ability to measure target range reliably and with low noise is paramount.

Acknowledgements

The authors acknowledge the financial support of the Naval Postgraduate School Direct Research Fund with technical sponsorship by the Office of Naval Technology

References

- Abkowitz, M. A., "Stability and Motion Control of Ocean Vehicles," *M.I.T. Press*, 1969.
- Healey, A.J., "Model Based maneuvering Control for Autonomous Underwater Vehicles" Transactions Of ASME, *Journal of Dynamic Systems Measurement and Control*, forthcoming issue in 1992

Fossen, T. I., "Nonlinear Modeling and Control of Underwater Vehicles", *Dr. Ing. Thesis*, Norwegian Institute of Technology, Trondheim, 1991

Principles of Naval Architecture, Ed. J. P. Comstock, Society of Naval Architects and Marine Engineers, 1967.

Slotine, J. J. E., Coetsee, J. A., "Adaptive Sliding Mode Controller Synthesis for Non-Linear Systems," *International Journal of Control*, Vol. 42, No. 6, 1986.

Utkin, V. I., "Variable Structure Systems with Sliding Modes," *IEEE Trans. on Automatic Control*, Vol. AC-22, April 1977, pp 212-222

Yoerger, D. R., Slotine, J. J. E., "Robust Trajectory Control of Underwater Vehicles," *IEEE Journal of Oceanic Engineering*, Vol. 10, No. 4, October 1985, pp 462-470.

Yoerger, D. R., Newman, J. B., Slotine, J. J. E., "Supervisory Control System for the JASON ROV", *IEEE Journal of Oceanic Engineering*, Vol. 11, No. 3, 1986, pp 392-400.

Yoerger, D. R., Cooke, J.G., Slotine, J. J. E., "The Influence of Thruster Dynamics on Underwater Vehicle Behavior and Their Incorporation in Design", *IEEE Journal of Oceanic Engineering*, Vol. 15, No. 3, 1991, pp 167-179.

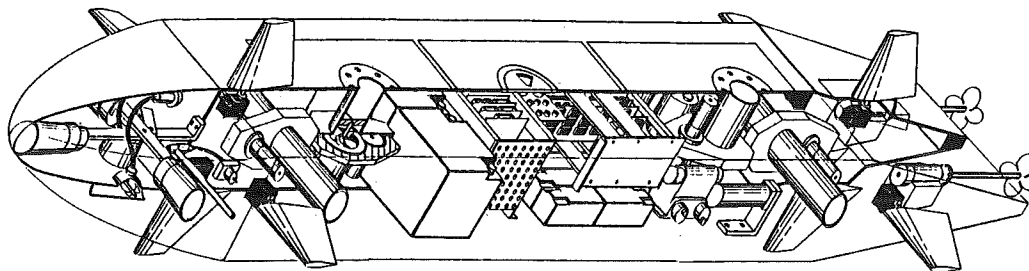


Figure 1 Sketch of the NPS AUV II Vehicle

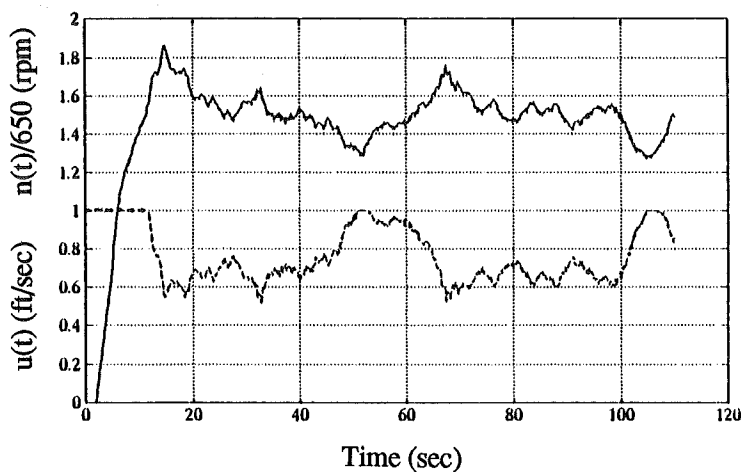


Figure 2a Response to Step Input of Speed

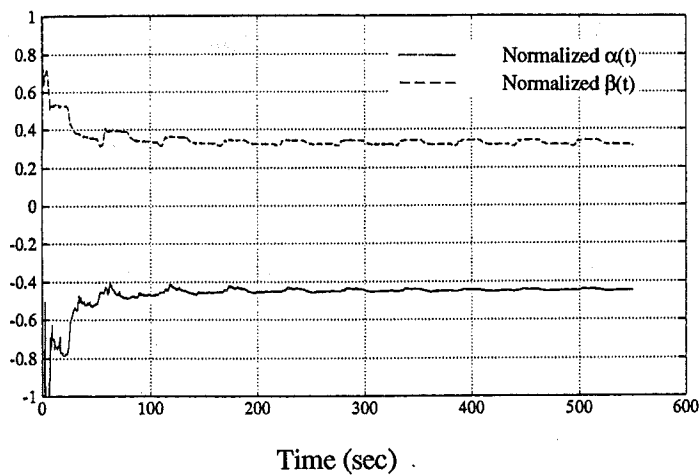


Figure 2b Identification of α and β using a Kalman Filter. Normalized $\alpha(t) = 18.8\alpha(t)$, Normalized $\beta(t) = 910,024\beta(t)$

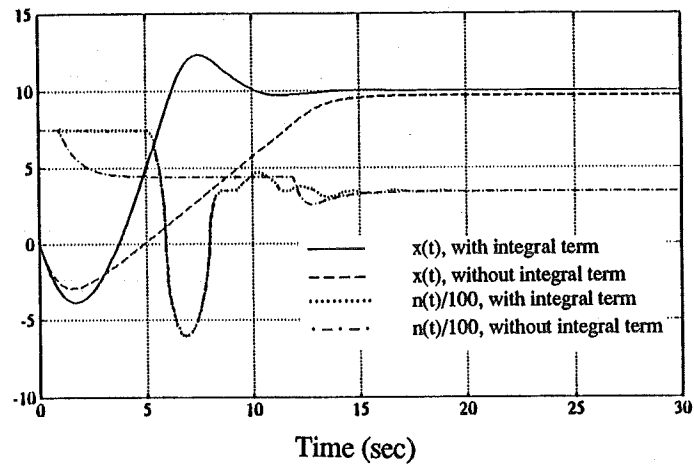


Figure 3 Response With and Without Integral Control

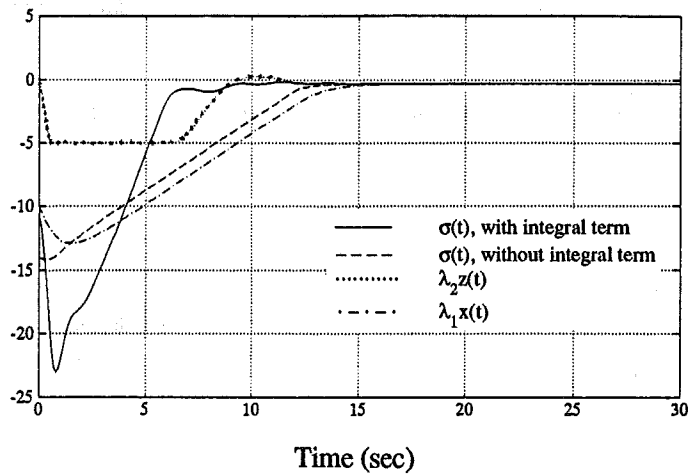


Figure 4 Behavior of Sliding Surface Terms

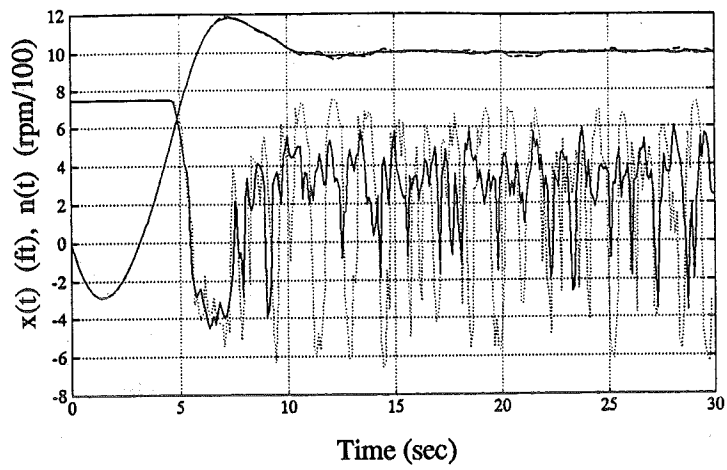


Figure 5 Response for Noise Levels of
 $-0.2 < v(t) < 0.2$ and $-0.5 < v(t) < 0.5$

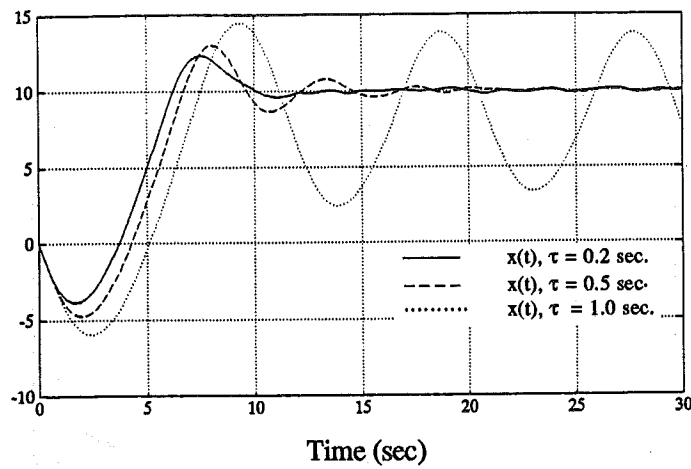


Figure 6 Response to Thruster Lags of
 $\tau = 0.2, 0.5,$ and 1.0

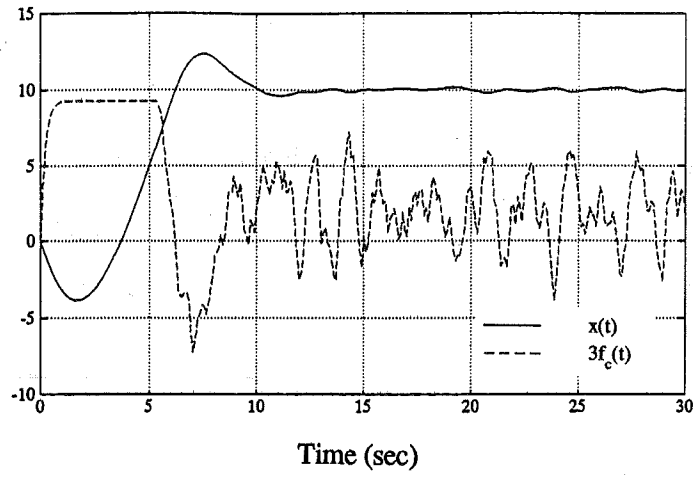


Figure 7 Position and Thruster Force for Noise Level of $-0.5 < v(t) < 0.5$

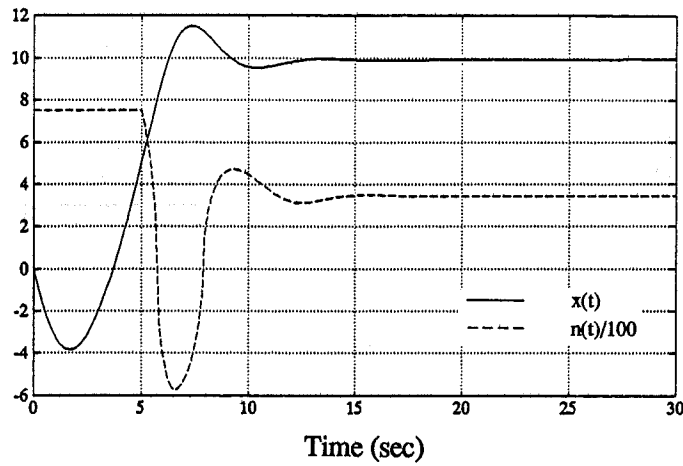


Figure 8 Response using a Slow Controller

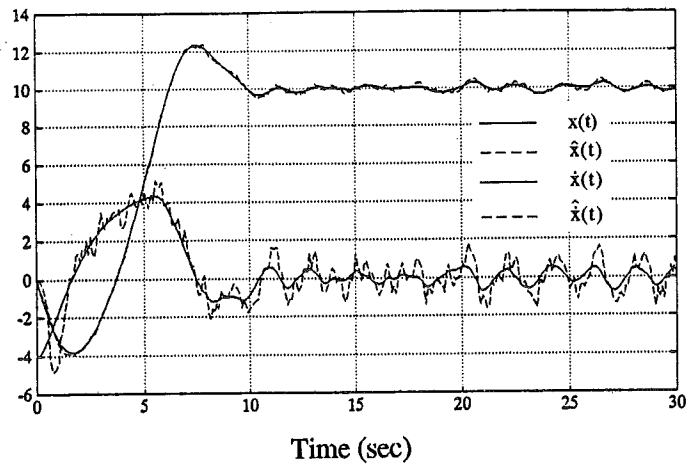


Figure 9 Response using a Fast Kalman Filter

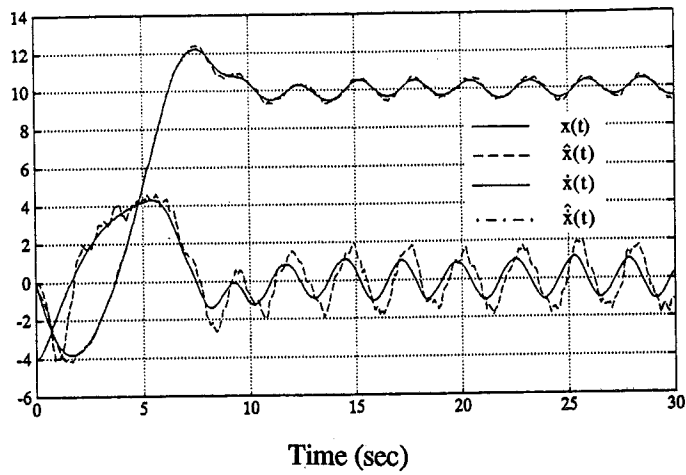


Figure 10 Response using a Slow Kalman Filter